Chemical Physics Letters 487 (2010) 62–66

Contents lists available at ScienceDirect

Chemical Physics Letters

journal homepage: www.elsevier.com/locate/cplett

X-ray reflectivity study of the adsorption of azacrown ether at liquid–liquid interface

Kamil Wojciechowski [a,*], Thomas Gutberlet [b], Aleksey Tikhonov [c], Kaoru Kashimoto [d,e], Mark Schlossman [e]

[a] Department of Microbioanalytics, Warsaw University of Technology, Noakowskiego 3, 00-664 Warsaw, Poland
[b] Forschungszentrum Jülich GmbH, Jülich Centre of Neutron Science, Lichtenbergstr. 1, 85747 Garching, Germany
[c] P.L. Kapitza Institute for Physical Problems, Russian Academy of Sciences, Kosygina 2, 119334 Moscow, Russia
[d] Department of Chemistry and Physics of Condensed Matter, Graduate School of Sciences, Kyushu University, Fukuoka 812-8581, Japan
[e] Department of Physics, University of Illinois at Chicago, Chicago, Illinois, USA

ARTICLE INFO

Article history:
Received 26 November 2009
In final form 14 January 2010
Available online 20 January 2010

ABSTRACT

Adsorption of diaza-18-crown-6 ether substituted with two tetracosane ($-C_{24}H_{49}$) alkyl chains (ACE-24) was investigated at the liquid–liquid interface. X-ray reflectivity measurements determined the structure of a close-packed monolayer at the hexane–water interface, which is consistent with conclusions drawn indirectly from earlier interfacial tension measurements on similar molecules. These data provide further insights into the role of interfacial processes involving azacrown ethers in ion separation techniques such as the permeation liquid membrane.

1. Introduction

Ion transfer through fluid–fluid interfaces plays a decisive role in many natural and industrial processes. One of the separation technologies relying on interfacial ion transfer is a permeation liquid membrane (PLM), where two aqueous solutions are separated by a hydrophobic membrane that is permeable only to selected chemical species, e.g. metal ions. The selectivity of transport is governed by complexing abilities of a carrier present in the membrane. PLM can be used for both industrial separations [1] and for analytical purposes [2,3]. Recently, the application of PLM as an environmental speciation sensor has been reported, e.g. by Zhang et al. [4]. The flux of metal ions through the PLM membrane provides an analytical signal, and information about the lability of the complexes present in the sample can be obtained [5]. In studies of Cu (II) transport in a PLM system developed by Buffle and coworkers the carrier consisted of a 1:1 mixture of an alkylated azacrown ether (N,N-didecyl-diaza-18crown-6 ether, ACE-10) and lauric acid (LAH) or palmitic acid (PAH), see Fig. 1. Previously, we have shown that both ACE-10 and the fatty acid molecules participate actively in transport of Cu (II) through the PLM membrane [6]. While LAH (or PAH) is a primary carrier for Cu (II) in the bulk of the membrane, ACE-10 plays an important role in the interfacial processes in transport of Cu (II), Pb (II) and Cd (II) ions [7]. Thanks to its high surface activity at liquid–liquid interfaces, ACE-10 is expected to easily form a close-packed monolayer, to which both Cu (II) and LAH are attracted, eventually forming a ternary Cu (II)-carboxylate-azacrown ether complex that is transported through the membrane [8].

Interfacial tension measurements at liquid–liquid [9] and liquid–gas [10] interfaces determined the surface activity of ACE-10 and its interaction with LAH within the monolayer. According to fits of the interfacial tension isotherm to the two-state reorientation model of Fainerman et al. [11] the ACE-10 molecules at organic–water interface were found to adopt one of two possible conformations, depending upon the actual value of surface pressure [9]. The interfacial tension results cannot, however, provide any direct information on the structure of azacrown ether monolayers, except the average area per molecule projected onto the surface in both states. For anisotropic and flexible ACE-10 molecules, it was speculated that the two possible adsorption states at the interface consist of alkyl chains perpendicular or parallel to the interfacial plane.

In this Letter we report on the study of the adsorption of a long chain ACE homologue, tetracosane alkylated diaza-18-crown-6 ether (ACE-24) at the liquid–liquid interface using X-ray reflectivity (XR). We chose to study a longer chain azacrown ether for our first experiment on these materials because the resultant thicker monolayer would allow for higher spatial resolution in the analysis of the X-ray measurements. Although structural differences between ACE-10 and ACE-24 can be expected, we leave the more challenging task of studying ACE-10 for future studies. X-ray reflectivity data probes the electron density of the adsorbed monolayer in the direction normal to the interface [12]. The technique is analogous to neutron reflection, which probes the neutron scattering length along the interfacial normal. Although neutron reflectivity offers the possibility of contrast variation to emphasize certain

* Corresponding author.
E-mail address: kamil.wojciechowski@ch.pw.edu.pl (K. Wojciechowski).

0009-2614/$ - see front matter © 2010 Elsevier B.V. All rights reserved.
doi:10.1016/j.cplett.2010.01.017

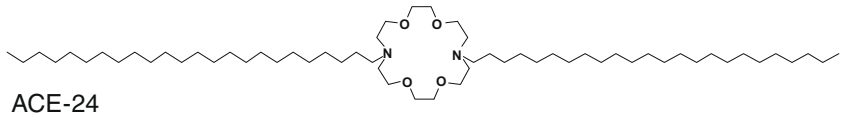

Fig. 1. Chemical structure of the azacrown ether ACE-24.

regions of the interface or molecules, it lacks the broad Q_z-range of X-ray reflectivity [13]. These have been successfully used to investigate the structure of adsorbed layers at the water–air interface and at buried interfaces between water and oil [14–19].

2. Experimental

2.1. X-ray reflectivity measurements

Experiments were carried out on the liquid surface scattering reflectometer at the X19C beamline, National Synchrotron Light Source (NSLS), Brookhaven National Laboratory, and at Sector-15 (ChemMatCARS) of the Advanced Photon Source (APS), Argonne National Lab, though the data illustrated in this Letter was measured at the APS. The reflectivity data consist of measurements of the X-ray intensity reflected from the sample interface normalized to the incident intensity with background subtracted as described previously [20,21]. The reflectivity is measured as a function of the wave vector transfer normal to the interface, $Q_z = (4\pi/\lambda)\sin\theta$, where λ is the X-ray wavelength ($\lambda = 0.79217 \pm 0.00005$ Å at the APS) and θ is the angle of reflection. X-ray reflectivity data were modeled using the Born approximation [22], though comparison fitting with the Parratt recursion method [23] yielded nearly identical fits.

The X-ray sample cell is a stainless steel chamber with Mylar windows, which allows the X-ray beam to pass through the upper phase (the hexane solution) [24] and then reflect off a hexane–water interface of area 76×100 mm (along the X-ray beam by transverse). In the experiment, the azacrown ethers spontaneously adsorb at this interface. The cell was cleaned with soap solution, methanol, and acetone, rinsed with Milli-Q water (Millipore Corp.), and then in purified hexane at 50 °C for 1 h. After partially filling the sample cell with 100 ml of water, and waiting for 15 min, the water surface was aspirated using a glass pipette connected to a vacuum pump. The hexane solution containing the azacrown ether (7×10^{-5} M) was then poured on top of the water subphase. The sample cell was sealed and left to equilibrate before further reflectivity measurements.

2.2. Interfacial tension measurements

Interfacial tension measurements were carried out using a drop profile analysis tensiometer PAT-1 (SINTERFACE Technologies, Germany). The drop profile analysis method is based on fitting the shape of the drop to the Gauss–Laplace equation from which the interfacial tension is calculated by means of the Axisymmetric Drop Shape Analysis Algorithm (ADSA) [25]. Details of the instrument have been described previously [26]. The surface purity of toluene was checked by measuring the dynamic interfacial tension (in water–air and water–organic system) overnight. All the glassware was thoroughly cleaned with Hellmanex II solution and rinsed with copious amounts of Milli-Q water. Measuring the dynamic interfacial tension of the solvent portion used for the last rinsing allowed the surface purity of all glassware to be checked prior to each use. For the azacrown ether solution, the interfacial tension was measured continuously for at least 3 h, each measurement was repeated three times or more. The equilibrium interfacial tension (γ_{eq}) was obtained using the long-term approximation of the Ward–Tordai equation [27].

2.3. Materials

N,N′-di-tetracosane-diaza-18crown-6 ether (ACE-24) was synthesized and purified as described previously [28]. Its purity was checked by measuring interfacial tension at the hexane–water and toluene–water interfaces. Hexane was purchased from Sigma Aldrich and purified by passing it through activated alumina in a chromatographic column. Toluene (puriss. p.a. ACS reagent for UV spectroscopy) was purchased from Fluka. Its surface purity was checked by measuring dynamic interfacial tension against Milli-Q water overnight. Hellmanex II surfactant solution used for cleaning the glassware was purchased from Hellma.

3. Results and discussion

3.1. Interfacial tension measurements

Our previous interfacial tension studies have shown that the toluene–water interface is completely covered with a monolayer of ACE-10 above a concentration of 10^{-3} M [9] and the high-coverage orientation (presumably with the alkyl chains perpendicular to the interface plane) starts to dominate at a bulk ACE-10 concentration of 3×10^{-5} M. Under typical PLM operating conditions ($C_{ACE\text{-}10} = 10^{-1}$ M), this orientation is thus dominant at the liquid–liquid interface. Therefore, the corresponding XR measurements should be performed under conditions of the maximum surface coverage, when the high-coverage orientation dominates the monolayer. On the other hand, increasing the surface coverage inevitably leads to a decrease of interfacial tension, in accordance with the Gibbs equation. As a consequence, capillary wave roughening of the surface increases, which smears out the molecular details of the interface probed by the X-rays. This problem becomes especially important in studying thin films of only few nm thicknesses, as in the present study. For this reason, the azacrown ether concentration of 7×10^{-5} M was used in this study. At this bulk concentration, our earlier interfacial tension measurements on ACE-10 indicated that a significant fraction of the interface is in the high surface coverage orientation [9], while the interfacial tension is still sufficiently high to keep the surface roughness low, as discussed below.

Preliminary interfacial tension studies with longer chain derivatives of azacrown ethers suggest that the presence of longer alkyl chains does not alter drastically their surface behavior. A long chain homologue azacrown ether was chosen for this study, possessing the same hydrophilic part as ACE-10 used in the original PLM, i.e. diaza-18-crown-6 ether, and differing only in the length of the alkyl chains substituted at the nitrogen atoms (see Fig. 1). The homologue with two $-C_{24}H_{49}$ alkyl chains (ACE-24) was synthesized according to the procedure described previously [28].

The interfacial tension drops from $\gamma = 51.4 \pm 0.3$ mN m^{-1} for a pure hexane–water interface to $\gamma = 33.0 \pm 0.4$ mN m^{-1} for the interface between water and a 7×10^{-5} M solution of ACE-24 in hexane at 22.8 ± 0.1 °C. Values of interfacial tension measured at the synchrotron using a Wilhelmy plate in the X-ray sample cell

are in good agreement with those obtained *ex-situ* using the drop-shape analysis method.

3.2. Surface roughness

The measured interfacial tension values γ were used to calculate the surface roughening due to capillary waves, according to the following formula [29,30]:

$$\sigma_{cap}^2 = \frac{k_B T}{2\pi}\int_{q_{\min}}^{q_{\max}} \frac{q dq}{\gamma q^2 + \Delta\rho_m g} \approx \frac{k_B T}{2\pi\gamma}\log\left(\frac{q_{\max}}{q_{\min}}\right) \quad (1)$$

where k_BT is the Boltzmann constant times the temperature, $\Delta\rho_m = 0.3453$ g cm^{-3} is the mass density difference of the two phases, g is the gravitational acceleration, $q_{\min} = (2\pi/\lambda)\Delta\beta\sin\theta$ (with the angular acceptance of the detector $\Delta\beta = 4.62\times10^{-4}$ rad [31]), and $\Delta\rho_m g = \gamma q_{\min}^2$. The variable q is the in-plane wave vector of the capillary waves. The limit, $q_{\max}$, is determined by the cutoff for the smallest wavelength capillary waves that the interface can support. We have chosen $q_{\max} = 2\pi/5$ Å^{-1} where 5 Å is an approximate molecular size. Note that σ_{cap} depends on $q_{\max}$ logarithmically and is not very sensitive to its exact value. At the highest Q_z of our X-ray measurements, the calculated capillary wave roughness $\sigma_{cap} = 4.35$ Å.

3.3. X-ray reflectivity measurements

The normalized X-ray reflectivity data R/R_F from the interface between the hexane solution of ACE-24 and water is shown in Fig. 2, where the Fresnel reflectivity, R_F, is calculated for an ideal interface in which the electron density profile between the hexane solution and the water is a step function. Variations in R/R_F from a value of 1 indicate the presence of interface roughening or additional structure due to, for example, molecules adsorbed at the interface. The solid line in Fig. 2 describes the primary features of the data and is the result of fitting a 2-slab model to the data [22]. Each slab represents a homogeneous layer of constant electron density that is sandwiched between the two adjacent phases. Each slab is used to represent a different part of the interface, such as the region occupied by the headgroup or the tailgroup of adsorbed ACE-24 molecules. When using this type of model, it is conventional to limit the number of slabs to the least number that provides a good fit to ensure that the fitting is not over-determined. In this case, a 1-slab model can produce a fit that is nearly as good as the one shown in Fig. 2. However, we have rejected this model because the electron density of a 1-slab model must be either smaller than that of hexane or larger than that of water in order to produce a normalized reflectivity R/R_F that immediately rises above $R/R_F = 1$ at small Q_z. Although this feature of the Fresnel curve is weak, we have consistently reproduced it when measuring different samples of alkylated azacrown ethers. Considerations of molecular packing and the structure of the ACE-24 molecule indicate that it is unphysical to assign to it an average electron density smaller than that of hexane or larger than that of water.

The 2-slab model that produced the solid line in Fig. 2 is represented by the electron density profile shown in Fig. 3. The dashed line indicates the underlying intrinsic electron density profile that is calculated with zero roughness (the two layers together represent an adsorbed monolayer of ACE-24, as described below). The two zero-roughness slabs have electron densities of 0.357 e$^-$ Å^{-3} and 0.253 e$^-$ Å^{-3} with corresponding thicknesses of 14 and 15 Å. The solid line is the electron density profile that is actually probed by the X-rays and includes the effect of roughness due to capillary waves. This roughness was fixed at the capillary wave value of 4.35 Å during the fitting procedure that yielded the profile shown in Fig. 3. When the roughness was varied over the range of 4.35 ± 0.4 Å, then variations in the other parameters are within one standard deviation of the fit indicated in Figs. 2 and 3.

The parameters of the model shown in Fig. 3 can be used to predict that the number of electrons per area in the monolayer of ACE-24 is given by 8.8 e$^-$ Å^{-2} (=14 × 0.357 + 15 × 0.253 e$^-$ Å^{-2}). If we assume that only ACE-24 molecules are in the interfacial region, then the fact that ACE-24 has 528 electrons allows us to calculate that the interfacial area per ACE-24 molecule is 60 Å^2. In the solid state, the area of a dodecyl-substituted azacrown ether (ACE-12) when lying flat on the interface is 90 Å^2 as determined by crystallographic measurements of its structure [32]. It should be noted that the size of the azacrown ether headgroup is independent of alkyl chain length, what allowed us to use the crystallographic data of a shorter chain ACE-12 derivative for the current discussion. An area per molecule of 60 Å^2 would indicate that the azacrown ether headgroups are tilted with respect to the interfacial normal by approximately 40°. This is qualitatively consistent with conclusions drawn from earlier interfacial tension measurements for alkylated crown ethers [33].

An area per molecule of 60 Å^2 is larger than the cross-sectional area of two close-packed all-trans alkyl chains (~40 Å^2). As a result, the tail group is likely to be disordered since the alkyl chains are not constrained to be close-packed. It is known that bulk alkyl chains just above their melting point, and therefore having the

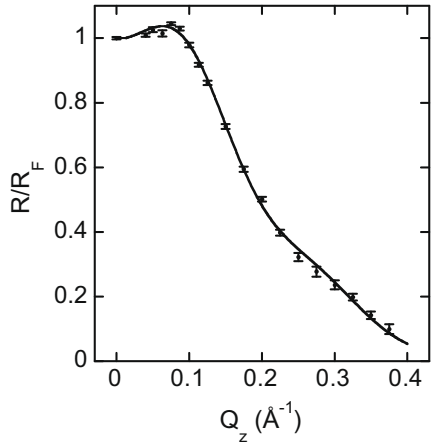

Fig. 2. Specular X-ray reflectivity normalized to the Fresnel reflectivity for the azacrown ether ACE-24 at the hexane–water interface at 22.8 °C. The solid line is a 2-slab fit discussed in the text.

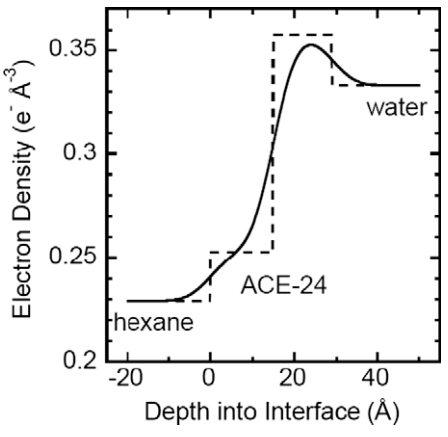

Fig. 3. Profile of the electron density (solid line) as a function of the depth into the interface for a layer of ACE-24 molecules adsorbed to the hexane–water interface. The dashed line illustrates the underlying electron density profile with a roughness of zero.

minimal disorder required for a liquid phase, have an electron density of about 0.270 $e^- Å^{-3}$ [34]. Also, a similar value of 0.266 $e^- Å^{-3}$ was measured for the electron density of disordered alkyl chains of long chain alkanols at the water/hexane interface [35]. These values are both slightly larger than the electron density of 0.253 $e^- Å^{-3}$ measured in the second slab further from the water subphase. Since the electron density of hexane is 0.230 $e^- Å^{-3}$, it is likely that hexane molecules intermixed with the ACE-24 molecules at the interface reduce the electron density of the second slab to its observed value.

If the interface was covered by close-packed azacrown ether head groups oriented parallel to the interface, then the expected electron density in the head group region would be 0.378 $e^- Å^{-3}$ [32], which is slightly larger than the measured value of 0.357 $e^- Å^{-3}$. When tilted from the normal, as described above, the azacrown ether head groups will extend in the normal direction about 10 Å. Given the 15 Å thickness of the first slab, we suggest that this thicker slab represents the head group region. The latter includes both the head groups, part of the alkyl chain closest to the head group, and possibly water and hexane intercalated in that region. The net result of these other molecules in the head group region would be to lower the electron density slightly. However, the present measurements do not have the resolution to distinguish the molecular details within this head group region. The success of the two-slab model is primarily a result of the large difference in electron densities between the region of the disordered alkyl tail groups and the higher average density of the head group region.

This molecular interpretation of our measured electron density profile suggests that there is a closely packed single layer of tilted ACE-24 molecules adsorbed at the hexane–water interface. We speculate that the region of the alkyl chains near the azacrown ether is likely to be more ordered than the region further away because of the geometric constraints imposed by the way the chains are attached to the azacrown ether. The maximum in electron density adjacent to the bulk water is due to the azacrown ether head group. The overall thickness of the two slabs is 29 Å, which is smaller than the ~37 Å that would be expected from an azacrown ether head group with all-*trans* $-C_{24}H_{49}$ alkyl chains projecting normal to the plane of the azacrown ether. The measured layer thickness provides further support for the presence of disordered tail groups in a tilted monolayer of ACE-24.

4. Conclusions

X-ray reflectivity measurements of the alkyl substituted diaza-18-crown-6 ether molecules at the liquid hexane–water interface reveal that azacrown ethers adsorb strongly and form a closely packed monolayer at the liquid–liquid interface. These data suggest that the azacrown ether head groups of the ACE-24 molecules are tilted with respect to the interfacial normal. The measured electron density profile indicates the presence of substantial disorder in the tail groups and the likelihood of hexane intermixing with the tail groups. This picture is in good agreement with the results of interfacial tension and neutron reflectivity (NR) for other alkylated azacrown ethers. NR results for partially deuterated ACE-16 suggest the presence of a second, loosely packed and diffuse layer of azacrown ether on the aqueous side of the hexadecane–water interface [36]. It should be, however, borne in mind that the aqueous solubility of the ACE-24 derivative is significantly smaller than that of ACE-16. As a result, in contrast to ACE-16, only the single, close-packed layer of ACE-24 derivative is observed at the liquid–liquid interface.

The present study suggests that the substituted azacrown ether used in the PLM studies indeed plays an important role in the mass transfer process through the liquid–liquid interfaces of PLM thanks to the formation of a closely packed structure at the membrane–aqueous interface. The closely packed monolayer of alkylated azacrown ether provides the interface with ion-recognition sites with selectivity governed by the coordination properties of the crown moiety. The process of ACE adsorption renders the PLM membrane–aqueous interface ion-selective and might play an important role in the overall selectivity of ion transport through membranes. An X-ray reflectivity study of the influence of the presence of transported metal ions on the structure of azacrown ether monolayers at the liquid–liquid interface is currently under way.

Acknowledgments

Financial support from the 374/N-COST/2009/0 and of COST Action D43 is acknowledged. K.K. acknowledges a fellowship from the Japan Society for the Promotion of Science. M.L.S. acknowledges support from the US NSF-CHE. ChemMatCARS is supported by the US NSF-CHE, NSF-DMR, and the US Department of Energy (DOE-BES). The Advanced Photon Source at Argonne National Laboratory and the National Synchrotron Light Source at Brookhaven National Laboratory are supported by the US DOE-BES. We thank Binhua Lin and Mati Meron for assistance with the X-ray measurements at ChemMatCARS.

References

[1] X.J. Yang, A.G. Fane, K. Soldenhoff, Ind. Eng. Chem. Res. 42 (2) (2003) 392.
[2] J. Buffle, N. Parthasarathy, N.K. Djane, L. Matthiasson, IUPAC Ser. Anal. Phys. Chem. Environ. Syst. 6 (2000) 407. In Situ Monitoring of Aquatic Systems.
[3] J.A. Jönsson, L. Mathiasson, J. Chromatogr. A 902 (1) (2000) 205.
[4] Z. Zhang, J. Buffle, H.P. van Leeuwen, K. Wojciechowski, Anal. Chem. 78 (16) (2006) 5693.
[5] N. Parthasarathy, J. Buffle, N. Gassama, F. Cuenod, Chem. Anal. (Warsaw) 44 (3A) (1999) 455.
[6] K. Wojciechowski, M. Kucharek, J. Buffle, J. Membr. Sci. 314 (1–2) (2008) 152.
[7] K. Wojciechowski, J. Buffle, R. Miller, Colloids Surf. A: Physicochem. Eng. Aspects 298 (1–2) (2007) 63.
[8] K. Wojciechowski, A. Bitner, G. Bernardinelli, M. Brynda, Dalton Trans. 7 (2009) 1114.
[9] K. Wojciechowski, J. Buffle, R. Miller, Colloids Surf. A: Physicochem. Eng. Aspects 261 (1–3) (2005) 49.
[10] K. Wojciechowski, D. Grigoriev, R. Ferdani, G.W. Gokel, Langmuir 22 (20) (2006) 8409.
[11] V.B. Fainerman, R. Miller, R. Wuestneck, A.V. Makievski, J. Phys. Chem. 100 (18) (1996) 7669.
[12] J. Als-Nielsen, D. McMorrow, Elements of Modern X-ray Physics, John Wiley and Sons Inc., Hoboken, 2001.
[13] J. Penfold, R.K. Thomas, D.J.F. Taylor, Curr. Opin. Colloid Interf. Sci. 11 (2006) 337.
[14] M.L. Schlossman, Phys. B: Condens. Matter (Amsterdam, The Netherlands) 357 (1–2) (2005) 98.
[15] S.V. Pingali, T. Takiue, G. Luo, A.M. Tikhonov, N. Ikeda, M. Aratono, M.L. Schlossman, J. Phys. Chem. B 109 (3) (2005) 1210.
[16] G. Luo et al., Faraday Discuss. 129 (2005) 23.
[17] S.V. Pingali, T. Takiue, G. Luo, A.M. Tikhonov, N. Ikeda, M. Aratono, M.L. Schlossman, J. Dispersion Sci. Technol. 27 (5) (2006) 715.
[18] M.L. Schlossman, A.M. Tikhonov, Annu. Rev. Phys. Chem. 59 (2008) 153.
[19] A. Goldar, S. Roser, A. Hughes, K. Edler, M.C. Gerstenberg, PCCP 4 (2002) 2379.
[20] D.M. Mitrinovic, S.M. Williams, M.L. Schlossman, Phys. Rev. E: Stat. Nonlinear Soft Matter Phys. 63 (1–2) (2001) 021601/1.
[21] M.L. Schlossman et al., Rev. Sci. Instrum. 68 (12) (1997) 4372.
[22] I.M. Tidswell, B.M. Ocko, P.S. Pershan, S.R. Wasserman, G.M. Whitesides, J.D. Axe, Phys. Rev. B 41 (1990) 1111.
[23] L.G. Parratt, Phys. Rev. 95 (1954) 359.
[24] D.M. Mitrinovic, Z. Zhang, S.M. Williams, Z. Huang, M.L. Schlossman, J. Phys. Chem. B 103 (11) (1999) 1779.
[25] M. Hoorfar, A.W. Neumann, Adv. Colloid Interf. Sci. 121 (2006) 25.
[26] G. Loglio, P. Pandolfini, R. Miller, A.V. Makievski, F. Ravera, M. Ferrari, L. Liggieri, Stud. Interf. Sci. 11 (2001) 439. Novel Methods to Study Interfacial Layers.
[27] A.V. Makievski, V.B. Fainerman, R. Miller, M. Bree, L. Liggieri, F. Ravera, Colloids Surf. A: Physicochem. Eng. Aspects 122 (1–3) (1997) 269.
[28] V.J. Gatto, K.A. Arnold, A.M. Viscariello, S.R. Miller, C.R. Morgan, G.W. Gokel, J. Org. Chem. 51 (26) (1986) 5373.

[29] A. Braslau, M. Deutsch, P.S. Pershan, A.H. Weiss, J. Als-Nielsen, J. Bohr, Phys. Rev. Lett. 54 (1985) 114.
[30] A. Braslau, P.S. Pershan, G. Swislow, B.M. Ocko, J. Als-Nielsen, Phys. Rev. A 38 (1988) 2457.
[31] D.M. Mitrinovic, A.M. Tikhonov, M. Li, Z. Huang, M.L. Schlossman, Phys. Rev. Lett. 85 (3) (2000) 582.
[32] S.L. De Wall, L.J. Barbour, G.W. Gokel, J. Phys. Org. Chem. 14 (7) (2001) 383.
[33] S. Ozeki, T. Ikegawa, S. Inokuma, T. Kuwamura, Langmuir 5 (1) (1989) 222.
[34] D.M. Small, The Physical Chemistry of Lipids, Plenum, New York, 1986.
[35] A.M. Tikhonov, S.V. Pingali, M.L. Schlossman, J. Chem. Phys. 120 (24) (2004) 11822.
[36] A. Zarbakhsh, J.R.P. Webster, K. Wojciechowski, Langmuir 25 (2009) 11569.